

Performance measurements on WISC collectors under artificial environmental conditions

S Pauletta^{1, *}, A Duret¹, G Dupont¹ and X Jobard¹

¹ Haute Ecole d'Ingénierie et de Gestion du Canton de Vaud (HEIG-VD), Yverdon-les-Bains, Switzerland

* Corresponding author: stefano.pauletta@heig-vd.ch

Abstract In the framework of the TriSolHP project, aimed at estimating the impact of improved heat pump technologies for decarbonization of non-retrofitted multifamily buildings in urban districts, a new type of PVT WISC (a photovoltaic-thermal wind and/or infrared sensitive collector) has been extensively tested in a climatic room without light input. The measurement campaign focused on the impact of airflow over the collector heat transfer coefficient for different installation layouts and when covered in ice. Measurement data were compared to TRNSYS simulations to gain an insight over the uncertainties affecting the performance models available in literature for this type of WISC.

1. Introduction

Photovoltaic-thermal (PVT) solar collectors combine the use of photovoltaic and solar thermal energy in a single component [1]. Usually consisting of covered or uncovered photovoltaic cells in close connection with a heat-extraction circuit, this type of component is designed to harness unused solar energy from photovoltaic cells, since more than 70 percent of incident solar radiation is converted into heat and about 20 percent into electricity [1]. Furthermore, the heat extracting circuit lowers the PV module temperature, thus enhancing the electricity production.

By equipping the back of a PV collector with an air-liquid finned heat exchanger, the design can be optimized to harness energy from the surrounding environment [2]. This type of collector can be adopted as a low-temperature energy source for heat pump systems in residential applications to provide the energy needed for heating and hot water production, even at night. In multifamily applications, this solution may have advantages over air-to-water heat pumps because of the noise problems of the latter technology. The greater dependence on environmental conditions of such a collector, on the other hand, complicates the adoption of a thermal performance model to properly estimate its energy performance, for example, during the planning phase of a construction project.

As part of the TrisolHP project, aimed at estimating the impact of improved heat pump technologies for decarbonizing unrenovated multifamily buildings in urban neighborhoods, one such PVT collector was tested extensively under artificially controlled environmental conditions and in the absence of light. The measurement data were then compared with simulation results calculated from three performance models available in the literature to understand the overall uncertainties and assist the choice of the model to use for future system-level calculations involving this type of collector.

2. A PVT WISC optimized for heat transfer with the environment

The PVT collector considered in the TriSolHP project is shown in Figure 1a. Manufactured by Consolar Solare Energiesysteme GmbH, the SOLINK collector is a 2 m² uncovered hybrid solar panel designed



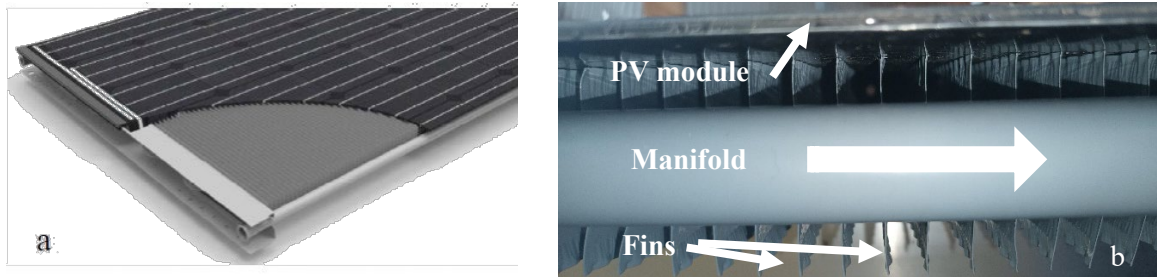


Figure 1. (a) Solink PVT collector (b) finned heat exchanger installed on its rear.

to operate with brine-water heat pumps. The heat exchanger on the underside of the collector (Figure 1b) integrates solar energy collection with energy from the surrounding air. In fact, the heat exchanger on the bottom side results in an area ten times larger than that of the module, increasing heat transfer to the environment and the sensitivity of the collector to wind [2]. This type of collector, once referred-to as “liquid-cooled uncovered collectors without rear isolation”, is now grouped with other types of PVT collectors under the name WISC (Wind and/or Infrared Solar Collector [3]).

2.1. Thermal performance model

Most PVT collectors or the embedded PV modules are certified in accordance with IEC 61215 (for crystalline silicon PV modules) and IEC 61730 safety qualification [1] to derive the electrical performance parameters of the collector. The electrical performance of the PVT collector can then be estimated by adopting the resulting electrical performance coefficients together with the corresponding electrical model.

The thermal performance of PVT collectors, on the other hand, is often measured according to the ISO9806 standard or its predecessor EN12795-2 as part of the Solar Keymark, an internationally recognized quality label for solar thermal collectors. The current standard allows two tests methods to be followed (quasi-dynamic and steady state, [3]), and considers a generalized model, in which some coefficients are set to zero depending on the collector under consideration. In previous versions of the test standard (the older EN12795-2 and the ISO9806:2014) the model was chosen based on the type of collector under test [1]. A series of relationships between the coefficients of the different models allows the parameters of the current model to be linked to those measured in an earlier version of the standard.

2.2. Model parameters for the Solink PVT collector

Table 1 shows 3 different sets of performance parameters derived from two Solar Keymark tests to which the Solink PVT collector was subjected (SK1 in 2019 and SK2, in 2021), and from field tests at the ISFH (F1, [4]): $\eta_{0,b}$ (dimensionless) is the zero-loss efficiency, based on beam irradiance; b_1 is the heat loss coefficient of the collector, in $[\text{W}/\text{m}^2/\text{K}]$; b_2 is the wind dependence of the heat loss coefficient, in $[\text{J}/\text{m}^3/\text{K}]$; b_u is the wind dependence of the conversion factor, in $[\text{s}/\text{m}]$; $(\text{Mc}_p)_{\text{eq}}$ is the equivalent heat capacity, in $[\text{kJ}/\text{m}^2/\text{K}]$. Although the ISO9806 standard indicates the level of accuracy with which to perform the measurements, it does not provide any method for determining the uncertainty of the curve parameters shown in Table 1. As a reference, calculations based on ad-hoc methodologies for a generalized flat-plate collector yield uncertainties of the order of 1% on the value of $\eta_{0,b}$ and 10% on the value of b_1 [5].

Constraints on environmental conditions during testing vary to some extent among model versions. Especially important for WISC collectors, wind speed and uniformity conditions are well defined and constrained, with a minimum wind speed during testing of 3 ± 1 m/s and an air speed measurement accuracy of ± 0.5 m/s. However, since these constraints are not always met in real life, the uncertainty on system-level simulation results increases.

Table 1. Sets of parameters available in literature for the PVT Solink collector.

Parameter set ID	Set 1	Set 2	Set 3	Units
Model source	* SK 1	* SK 2	¹ F1	-
$\eta_{0,b}$	0.468	0.137	0.532	-
b_1	22.99	84.35	19.08	W/m ² /K
b_2	7.57	22.03	3.69	J/m ³ /K
b_u	0.144	0.810	0.126	s/m
$(Mc_p)_{eq}$	26.05	41.58	26.05	kJ/m ² /K

* SK: Solar Keymark certification

¹ F1: field test performed at the Institute for Solar Energy Research in Hamelin (ISFH)

Table 2. Sensor accuracy and environmental control uncertainties.

Measurement/ sensor/ units/ sampling	Uncertainty@3 σ	Control stability@3 σ
Air temperature T_{air} / PT100 B Class/ [°C] / 5 s	± 0.5 K	± 0.75 °C
Air relative humidity, H_{air} / Combo H+T/ [%] / 5 s	± 10 %	± 10 %
Air speed v_{wind} / GILL, Windmaster / [m/s] / 1 s	± 1.5 %	± 0.75 m/s
HTF temperature: T_{in} , T_{out} / PT100 1/3 DIN/[°C]/ 25 s	± 0.1 K @ 0°C	± 0.03 °C
HTF flowrate, \dot{W}_{HTF} / Khrono Optiflux/ [l/h]/ 25 s	± 1.5 % @ 50 l/h ± 0.75 % @ 125 l/h	± 1 l/h

3. Measurements performed under artificial environmental conditions

Given the environmental conditions encountered in Switzerland during winter nights, an important issue is understanding the behavior of the collector under freezing conditions and when the collector is covered by an ice layer. Particularly, if a heat pump system equipped with this type of collector is intended to be the sole heat generator, the PVT collectors must cover the energy demand of the heat pump even under extreme conditions. To clarify this issue and adopt the best available model for future calculations, a series of measurements were made in a climatic room without light to simulate the performance of SOLINK during freezing and under varying environmental conditions at night.

3.1. Instrumentation and measurement setup

The measurement campaign took place in the climatic room of the Haute Ecole d'Ingénierie et Gestion du Canton de Vaud (HEIG-VD). Featuring a 100 m³ useful volume, the climatic room allows a temperature range of -10°C to 60°C to be established, ensuring a maximum air flow rate of 12,000 m³/h. During testing, once stable ambient conditions are reached, a 40% v/v glycol mixture (called Heat Transfer Fluid, or HTF) is circulated through the manifold, measuring its volumetric flow rate and inlet and outlet temperature. Ambient conditions are characterized by measuring the air velocity at 5 cm above the collector panel, along with the temperature and humidity of the circulating air. Table 2 lists the main characteristics of the measurement equipment, its accuracy and uncertainties related to the control of test conditions in the climatic room.

3.2. Test conditions

During the campaign, several tests were planned and performed under different conditions. During the ice formation test, the temperature inside the climatic room was maintained at 0°C, while the HTF inlet temperature and the air relative humidity were kept at -10°C and over 85%, respectively. The circulating

HTF was maintained constantly at around 50 l/h, and the collector was installed on a freestanding structure for installation on a flat roof with a 45° tilt and oriented upwind. During air velocity tests, performance measurements were again made on the freestanding structure oriented upwind but with an inclination of 20°, with air at 15 °C and relative humidity of 40-50% (to avoid water condensation), an HTF inlet temperature of 5°C and a flowrate of about 80 l/h. To assess the impact of collector orientation and installation type on its performance, measurements were made for 3 installation layouts (freestanding structure with 20° tilt, east-west structure with 25° tilt, and sloped roof integration) and for 5 orientations with respect to inlet airflow (0°, 45°, 90°, 135° and 180° - see Figure 2) while maintaining climatic conditions that prevented water condensation on the collector. During all the tests, moreover, the air temperature was assumed in equilibrium with that of the chamber walls and was adopted as the "sky temperature" in the performance models used in the following data analysis.

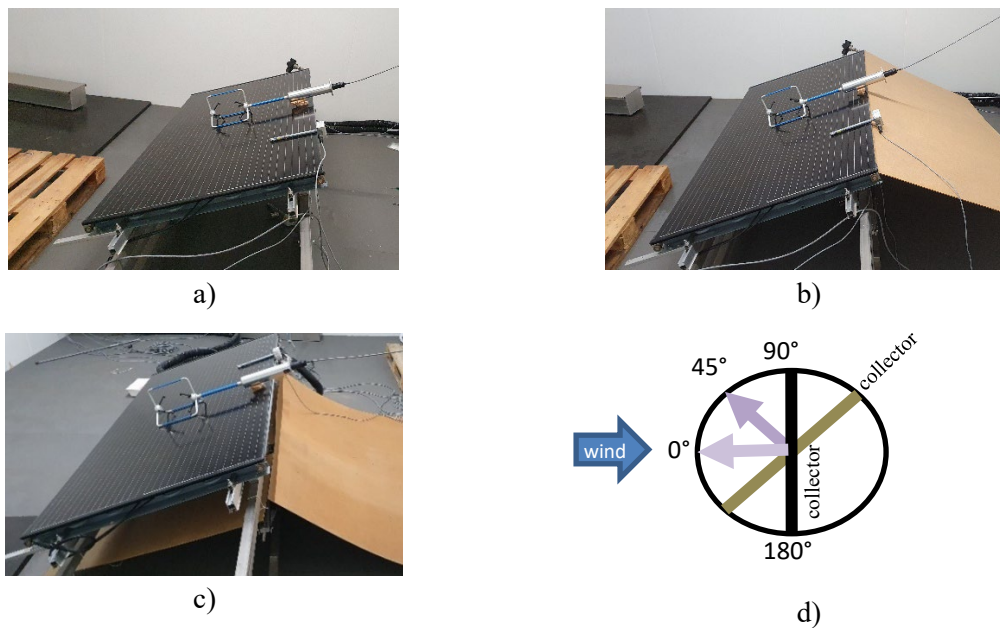


Figure 2. Collector layout and orientation tested during measurements: a) freestanding structure at 20° tilt; b) an east-west structure at 25° tilt; c) model for sloped roof integration; d) convention used for collector orientation (i.e., when at 180°, the air flows over the rear of the collector first).

3.3. Measurement results

The collected heat flux \dot{q}_{ccl} , in [W/m²], and the heat transfer coefficient referred to the collector front area U_{ccl} , in [W/m²/K], were calculated to compare measurement data to model estimates based on the following equations, valid for periods when the collector temperature was constant (or slowly changing):

$$\dot{q}_{ccl} = \frac{\dot{m}c_p}{A_G} (T_{out} - T_{in}) \quad (1) \quad U_{ccl} = \frac{\dot{q}_{ccl}}{(T_a - T_m)} \quad (2)$$

where \dot{m} , in [kg/s], is the mass flow rate through the collector; c_p is the HTF specific heat, in [J/kg/K]; A_G is the collector pane gross area, in [m²]; T_{in} and T_{out} are, respectively, the HTF temperature at the inlet and at the outlet of the PVT collector, in [K]; while T_a and T_m are, respectively, the ambient and the mean collector temperatures, in [K].

3.4. Ice formation test

During the ice formation test, the temperature of the test room was kept below zero in the presence of high humidity (left box in Figure 3). Over the 96 hours of continuous freezing conditions (right box in Figure 3), the collector became increasingly covered with ice and its heat transfer with the environment decreased, from a U-value of more than 24 W/m²/K to less than 19 W/m²/K (+/- 2 W/m²/K at 1 σ), a

25% reduction in value. Given the extreme conditions to which the collector was exposed and the duration of the test, it can be concluded that the collector can provide a relevant fraction of the available ambient energy, even when covered by ice, and heat pump systems equipped with this type of collectors might not require defrosting cycles.

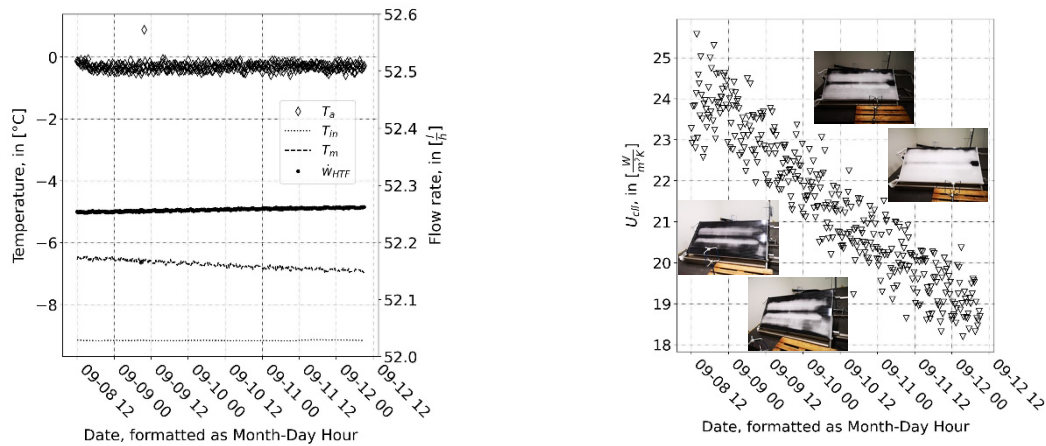


Figure 3. Climatic conditions in the test room (left) and overall heat exchange coefficient (right) measured during the ice formation test.

3.5. Influence of air velocity

The performance of the PVT collector was tested under varying airflow to study the impact of air velocity on the heat transfer coefficient at night with no irradiance. Figure 4a confirms that the energy transfer from the environment increases with increasing air velocity, as the heat exchange rate between the HTF and the outside air increases. Given that if solar radiation were present temperature gradients over the PV panel would enhance air turbulence, these values should provide an estimate of the minimum heat transfer coefficient of the PVT for air velocities larger than 0.8 m/s (i.e., ~3 km/h).

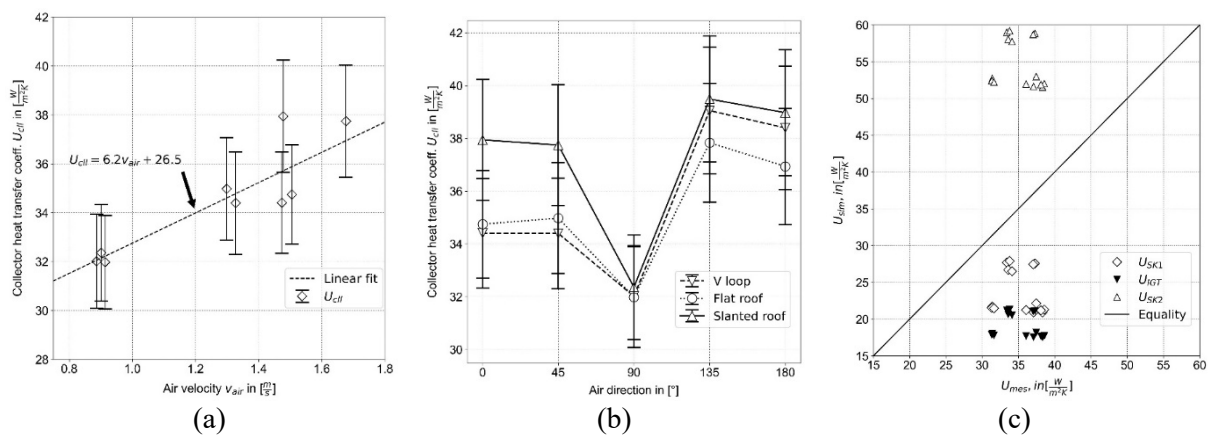


Figure 4: a) Collector $U_{c,eff}$ versus air velocity; b) collector $U_{c,eff}$ for several orientations and layouts; c) comparison between measured and simulated $U_{c,eff}$ of the PVT WISC under test.

3.6. Influence of the installation layout and collector orientation

To study how the collector performance is affected by the installation layout, measurements were made on 3 types of installations: a freestanding structure for flat roof; a west-east layout; and a sloped roof integration (see Figure 2). In each case, 5 different orientations with respect to airflow were tested, using the convention that 0° indicates that the airflow is over the front and 180° over the back of the collector. As Figure 4b shows, the transfer coefficient between the PVT manifold and the environment increases

with increasing incidence over the rear fins, with a minimum in all tested cases when the airflow is perpendicular to the fins at the rear of the manifold (i.e., 90° orientation). In this arrangement, airflow in the rear fin channels decreases considerably, hindering the collector's exchange with the surrounding air. When air flow comes from the front, on the other hand, it can also flow under the collector, increasing air turbulence at the rear fins. In the case of roof integration, in particular, the constant "channel" between collectors and roof forces the flowing air, maintaining its speed and turbulence over the rear fins. By contrast, in the case of east-west installation or for freestanding structures, air reaching the rear side flows into a plenum and slows down, decreasing the collector heat transfer.

3.7. Comparison with thermal performance models

The measurement data were finally compared to the results of TRNSYS simulations adopting the "type 203" (see [6]) and the various parameters of Table 1, to evaluate which set is more reliable for future calculations focused on system-wide simulations. Figure 4c shows the comparison between the measured collector overall heat transfer U_{cl} and the simulated ones. It is evident how the parameters derived from the new Solar Keymark certificate, issued in 2021, overestimate the collector U by a significant amount (more than 50%). The other models, on the other hand, derived from the preceding Solar-Keymark certificate (SK1, issued in 2019) and from the field test at the ISFH [4], underestimate the collector U by more than 20 and 40%, respectively.

4. Conclusions

PVT collectors with enhanced sensitivity to the environment can be adopted as the sole low temperature energy source in water/brine heat pump applications, but the modeling of their thermal performance is affected by uncertainties linked to the standard followed during testing. Measurements under controlled environmental conditions have allowed investigating the effect of air velocity and installation layout for the case of a PVT WISC under investigation at the HEIG-VD. By comparing measurement data to the results of TRNSYS simulations performed with three different performance models, it is concluded that the parameters derived from the first Solar Keymark certification are better suited to describe the collector thermal performance and they will be adopted for future system-wide simulations. The results of an ice formation test, lastly, allow one to be confident that even in extreme weather conditions and under a thick layer of ice this type of collector will allow extracting from the environment a relevant fraction of the available heat.

References

- [1] Zenhäusern D, Bamberger E, Baggenstos A, and Häberle A. (2017) PVT Wrap-Up: Energy systems with photovoltaic-thermal solar collectors - Technology, market, experiences *Proc. ISES Solar World Congress 2017*, Abu Dhabi UAE.
- [2] Littwin M, Lampe C, Kirchner M, Chhugani B, Pärtsch P and Giovannetti F (2021) *TwinPower - Integrierte Gesamtenergieversorgung von Wohngebäuden mit PV-thermischen Kollektoren als bisolare Wärmepumpenquelle* Institut für Solarenergieforschung Hameln GmbH (ISFH).
- [3] Bohren A. (2017) Report from ISO 9806:2017 - The new collector standard *ESTESC Webinar 2017*.
- [4] Chhugani B, Pärtsch P, Kirchner M, Littwin M, Lampe C and Giovannetti F (2020) Model validation and performance assessment of unglazed photovoltaic-thermal collectors with heat pump systems *ISES Conference Proc. (2020)* Chennai India.
- [5] Sabatelli V, Marano D, Braccio G and Sharma V K (2002). Efficiency test of solar collectors: uncertainty in the estimation of regression parameters and sensitivity analysis. *Energy Conversion and Management*, 43(17). [https://doi.org/10.1016/S0196-8904\(01\)00180-7](https://doi.org/10.1016/S0196-8904(01)00180-7).
- [6] Stegmann M, Bertram E, Rockendorf G, Janßen J (2011) Model of an unglazed photovoltaic thermal collector based on standard test procedures *30th ISES Biennial Solar World Congress 2011* (Vol. 4) SWC 2011 pp. 2639–2647.